Journal of Materials and Environmental Sciences
ISSN : 2028-2508
CODEN : JMESCN

J. Mater. Environ. Sci., 2018, Volume 9, Issue 9, Page 2567-2574

http://www.jmaterenvironsci.com

Solution Combustion Synthesis, Characterization and Photocatalytic Activity of α-Fe_2O_3 Nanopowder

M. N. Zulfiqar Ahmed [1], K. B. Chandrasekhar [2], A. A. Jahagirdar [3], H. Nagabhushana [4], B. M. Nagabhushana [5*]

1. Research Scholar, Jawaharlal Nehru Technological University Anantapur, Anantapuramu -515002, India2. Department of Chemistry, Jawaharlal Nehru Technological University Anantapur, Anantapur - 515002, India
3. Department of Chemistry, Dr. Ambedkar Institute of Technology, Bangalore - 560056, India
4. Department of Postgraduate Studies and Research in Physics, Tumkur University, Tumkur - 572 103, India
5. Department of Chemistry, M.S. Ramaiah Institute of Technology, Bangalore - 560054, India

Received 20 Jun 2016,
Revised 17 Oct 2016,
Accepted 23 Oct 2016

Keywords

- ✓ α-Fe_2O_3;
- ✓ Acid orange 7;
- ✓ BET surface area;
- ✓ Photocatalytic activity;
- ✓ Photocatalyticactivity

B. M. Nagabhushana
q3c5@yahoo.com
+918023600822

Abstract

The paper describes the synthesis of α-Fe2O3 nanopowder solution combustion synthesis. The nanopowder was characterized by powder X-ray diffraction (PXRD), Fourier transform infrared spectroscopy (FTIR), scanning electron microscopy (SEM) and band gap energy measurements. The nanopowder exhibited the hexagonal phase of α-Fe2O3 as indicated by the PXRD pattern. The nanopowder was used photocatalyst for the removal of the dye acid orange 7 (AO 7) from its aqueous solution. The effect of various factors such as initial dye concentration, dosage of the photocatalyst and irradiation time on the rate of photocatalysis was also studied. It was found that the nanopowder exhibited good photocatalytic activity for the removal AO 7 from its aqueous solution.

1. Introduction

The presence of intensely colored effluents in the affects its quality and reduces the penetration of light. This results in disturbance of the biological processes occurring within the stream. Dyes are a class of synthetic organic compounds which cause coloration of the natural water bodies when released into the environment [1, 2]. The discharge of effluents from the dyeing industries has resulted in the need for treating the wastewaters with high values of biochemical and chemical oxygen demands as well as the color perceived by the human eyes at very low concentrations. The presence of unnatural color in water leads to its contamination and also makes it aesthetically unpleasant [3-5].

The organic groups present in the dyes produce certain reactive intermediates which trigger morphological and genetic alterations leading to cytotoxic and carcinogenic effects [6]. Besides possessing high stability in sunlight, dyes are resistant to microbial attack and temperature [7, 8]. The discharge of azo dyes into the water bodies produces toxic amines which are formed by the reductive cleavage of the azo linkages present in them. These toxic amines severely affect the vital organs of the body such as kidney, liver and brain. They also affect the reproductive and nervous systems. Dyes also contain aromatic compounds, chlorides, meals etc. which affect the photosynthetic activity of some aquatic organisms [9, 10].

A number of techniques are being used for the removal of dyes from solution. These include physical adsorption, chemical and wet air oxidation, nanofiltration, catalytic processes, reverse osmosis, electrochemical coagulation, biological treatment methods, precipitation and chemical degradation processes [11-14].

Most of the conventional methods are not being employed on a large scale due to the high cost ad problems associated with the disposal of sludge [15]. Photocatalysis is an important method involved in the removal of

traces of hazardous chemicals [16]. Several metal oxide semiconductors such as ZnO, α-Fe_2O_3, Fe_3O_4, SnO_2, Al_2O_3 etc. have been used for the removal of dyes from their aqueous solutions. Iron oxide has a narrow band gap energy of 2 to 2.2 eV and can absorb light upto 600 nm. It can collect 40% of the solar energy, less expensive and is stable in most of the aqueous solutions [17-21].

α-Fe_2O_3 nanoparticles exhibit certain unique characteristics such as high saturation fields, superparamagnetism and extra anisotropy contributions. These unique characteristics are the result of finite size and large surface area values of the nanoparticles. α-Fe_2O_3 nanoparticles find applications in different fields such as catalysis, magnetic storage devices, electrochemistry, biotechnology, medicine and so on [22-26].

The synthesis of α-Fe_2O_3 nanocrystals with different morphologies like belts, rods, nanorings, tubes, urchinlike, quasicubic, hollow spheres and nanorhombohedra has been reported in the literature [22, 27-33]. α-Fe_2O_3 nanopowders with average crystallite sizes of 35, 100 and 150 nm were prepared by thermal evaporation and co-precipitation methods [34]. The nanopowders were as photocatalysts for the removal of the dye Congo red under visible light irradiation. The α-Fe_2O_3 nanopowders with crystallite sizes 35 and 150 nm resulted in almost complete removal of the dye whereas the nanopowders with crytsallite size 100 nm did not decompose the dye.

Various methods are being employed for the synthesis of α-Fe_2O_3nanoprticles. Some of these methods include reduction of iron salts micelles, thermal reactions, electrochemical methods, microemulsion, co-precipitation, sol-gel and hydrothermal method [35-40]. Solution combustion synthesis yields high purity crystalline products with desired composition and structure in a short period of time [41]. The process is simple, cost effective and yields high quality product [42]. In the present work, α-Fe_2O_3 nanopowder was synthesized by solution combustion synthesis. The nanopowder was as photocatalyst for the removal of the dye Acid orange 7 (AO 7) from its aqueous solution.

2. Experimental Details

2.1. *Preparation of the nanopowder*

The chemicals required for the study were procured from sd Fine Chemicals Limited, India. The Ferric nitrate $Fe(NO_3)_3.9H_2O$ was used as the oxidizer and oxalyldihydrazide (ODH), $C_2H_6N_4O_2$ was used as the fuel. ODH was prepared by the methods described by Patil et al. [43]. A 1000 ppm solution of AO 7 was used as the stock solution. It was appropriately diluted with double distilled water to obtain solutions of concentrations 20, 40 and 60 ppm. All the chemicals were of analytical grade and were used without further purification. Double distilled water was used throughout the experiments.

5g of ferric nitrate was taken in a crystallizing dish of approximately 300 mL capacity and dissolved in minimum quantity of double distilled water. Calculated amount of ODH was added to it and the mixture was stirred magnetically for about 10 minutes to achieve uniform mixing. The excess water was evaporated by heating it over a hot plate. The crystallizing dish was then introduced into a muffle furnace maintained at around 350^0C. The reaction mixture first dehydrated, ignited at one spot and then burnt to to form the desired nanopowder. In order to achieve complete combustion, the oxidizer to fuel ratio was maintained at 1 (oxidizer/fuel = 1). Equation 1 represents the reaction between ferric nitrate and ODH to form the nanopowder [44].

$$Fe(NO_3)_3(aq) + 3C_2H_6N_4O_2(s) \longrightarrow Fe_2O_3(s) + 6CO_2(g) + 9N_2(g) + 9H_2O(g) \quad (1)$$

2.2. *Characterization of the nanopowder*

2.2.1 *XRD analysis*

The PXRD pattern of the nanopowder was recorded using Philips X-ray diffractometer (PW/1050/70/76) using Cu K_α radiation (λ = 1.542Å) at 30 kV and 20 mA with Ni filter. The mean crystallite size of the nanopowder was calculated using Scherer's formula represented by Equation 2 [45].

$$D = \frac{k\lambda}{\beta \cos\theta} \quad (2)$$

where D is the mean crystallite size, k is a constant, λ is the wavelength of X-rays used, β is the full width at half maximum (FWHM) and θ is the Bragg's angle.

2.2.2 *FTIR analysis*

The FTIR spectrum of the nanopowder was recorded by Nicolette IMPACT 400 D FTIR spectrometer from 300 to 4000 cm^{-1} using KBr as the reference sample.

2.2.3 *SEM analysis*
The SEM micrograph of the nanopowder was recorded using the JEOL (JSM-840A) scanning electron microscope.

2.2.4 *Band gap energy measurements*
The band gap energy of the nanopowder was determined by fitting the absorption data in the direct transition equation represented by Equation 3 [46].

$$(\alpha h\nu)^2 = A(h\nu - E_g) \quad (3)$$

where α is the optical absorption coefficient, (hν) is the energy of the photon, E_g is the band gap energy and A is a constant. $(\alpha h\nu)^2$ was plotted aw a function of hν and the linear portion of the curve was extrapolated to meet the photon energy axis. The value of E_g was determined from the intersection of the extrapolated linear portion of the X-axis.

2.3. *Photocatalytic activity of the nanopowder*
AO 7 is an anionic azo dye used in paper and textile mills. Earlier it was also used in tanneries. It has the molecular formula $C_{16}H_{11}N_2NaSO_4$ and molecular mass equal to 350.3 $gmol^{-1}$. Chemically, AO 7 is 4-[(2-hydroxy-1-naphthyl)azo]benzenesulfonate. It is highly toxic in nature. It causes nausea, dermatitis, methemoglobinemia; irritation of the eyes, skin, mucous membrane and the upper respiratory tract. AO 7 also exhibits carcinogenic effects [47-49]. The structure and absorption spectrum of AO 7 are given by Figures 1 and 2 respectively. The maximum absorbance was observed at 487 nm.

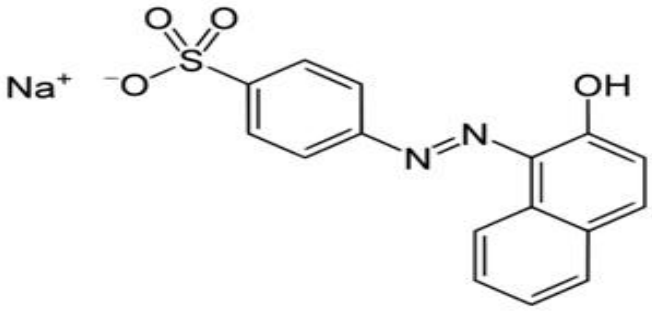

Figure 1. Structure of acid orange 7

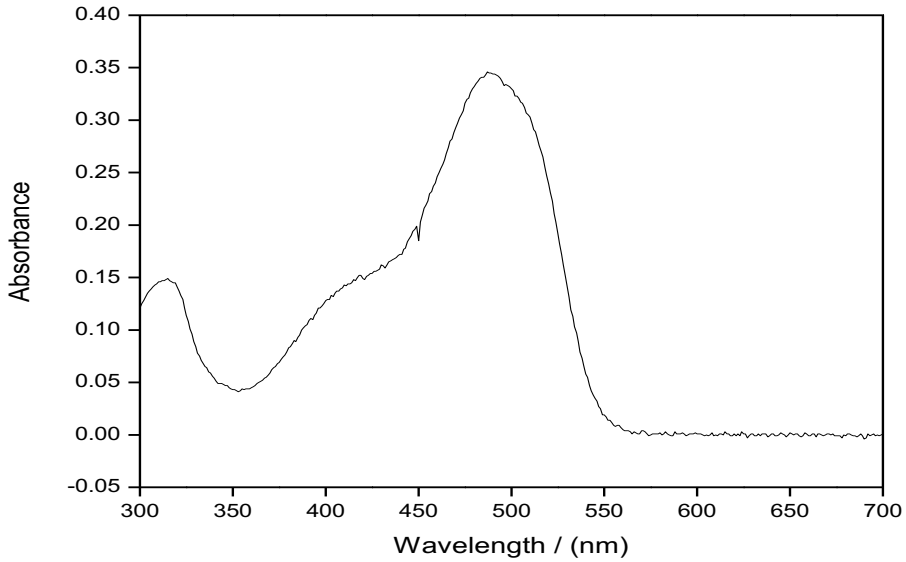

Figure 2. Absorption spectrum of acid orange 7

The reaction vessel used in the photocatalytic experiments had an exposure area of 50.3 cm^2 with a circumference of 25.2 cm. The source of Uv radiation was a 25 Watt mercury vapour lamp. A distance of about 20 cm was maintained between the source and the surface of the solution.

50 cm^3 of the AO 7 solution was transferred to the reaction vessel and appropriately amount of the nanopowder was added to it. The mixture was stirred magnetically for 30 minutes under Uv radiation and then centrifuged at 3000 rpm using the KEMI C8C centrifuge. The Uv-visible spectrum of the supernatant was recorded in the wavelength of 300 to 700 nm with the help of ELICO SL 159 spectrophotometer. The percentage dye removal was calculated using Equation 4 [50].

$$\% \, dye \, degradation = \frac{(C_0 - C_e)}{C_0} \times 100 \qquad (4)$$

where C_0 and C_e are the initial and equilibrium concentrations of the dye solution.

The experiments were conducted by varying the dosage of the nanopowder from 0.2 to 2.0 gL^{-1} of the dye solution. The optimum dosage was found by plotting the graph of C_e/C_0 versus the dosage of the nanopowder.

The effect of irradiation time was found as follows. 100 cm3 of the dye solution was taken in the reaction vessel, optimum dosage of the nanopowder was added to it and the mixture was stirred magnetically under Uv-light. After every 5 minutes, a small aliquot of the mixture was taken out, centrifuged and the Uv-visible spectrum was recorded as described earlier. The optimum irradiation time was recorded from the plot of C_e/C_0 versus the irradiation time.

The photocatalytic experiments were repeated for four initial concentrations of the dye solutions: 10, 20, 40 and 60 ppm.

3. Results and Discussion

3.1 *XRD analysis*

The peaks in the PXRD pattern of the nanopowder (Figure 3) were attributed correspond to the hexagonal phase of α-Fe_2O_3 with JCPDS file number: 84-0311 [51]. The PXRD pattern exhibited high degree of crystallinity with no impurity peaks.

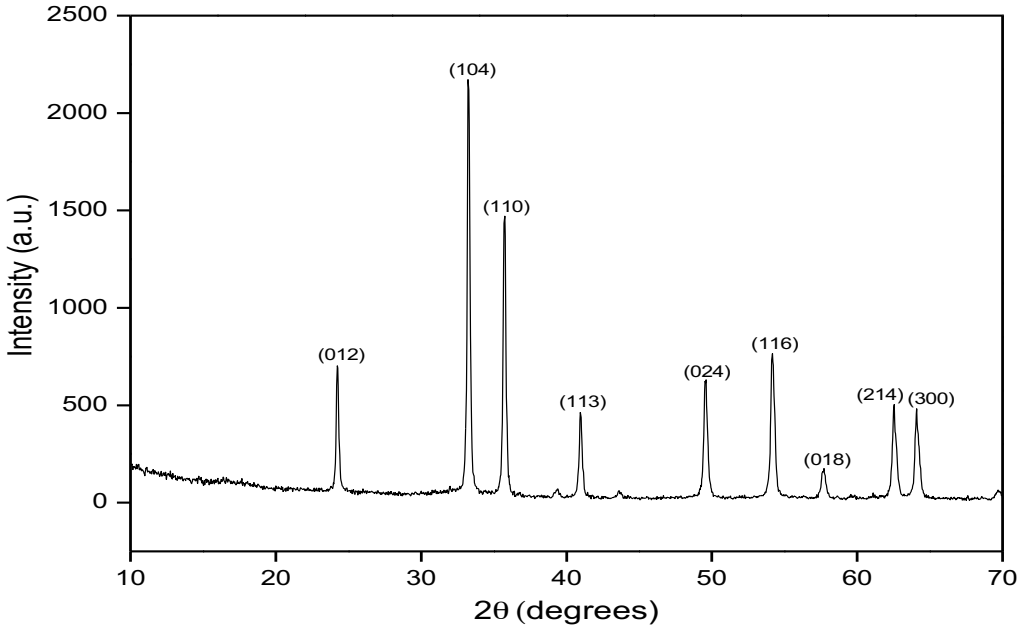

Figure 3. PXRD pattern of the nanopowder

3.2 *FTIR analysis*

The peaks around 416 and 542 cm^{-1} in the FTIR spectrum of the nanopowder shown in Figure 4 were assigned to the stretching vibrations of the Fe–O bond. The peak around 3400 cm^{-1} was attributed to be due the –OH group of water adsorbed on the surface of the nanopowder [52].

3.3 *SEM analysis*

Figure 5 shows the SEM micrograph of the nanopowder. The SEM micrograph indicated that the particles were agglomerated with a number of voids. The formation of voids was attributed to the large volumes of gases released during the combustion process. The agglomeration of the particles was considered as a common way by which they minimize their surface energy [53].

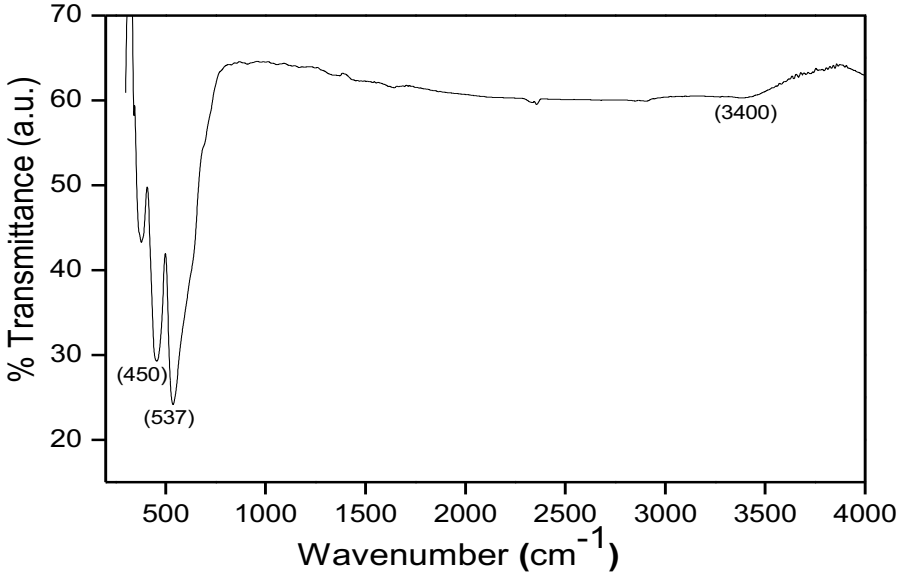

Figure 4. FTIR spectrum of the nanopowder

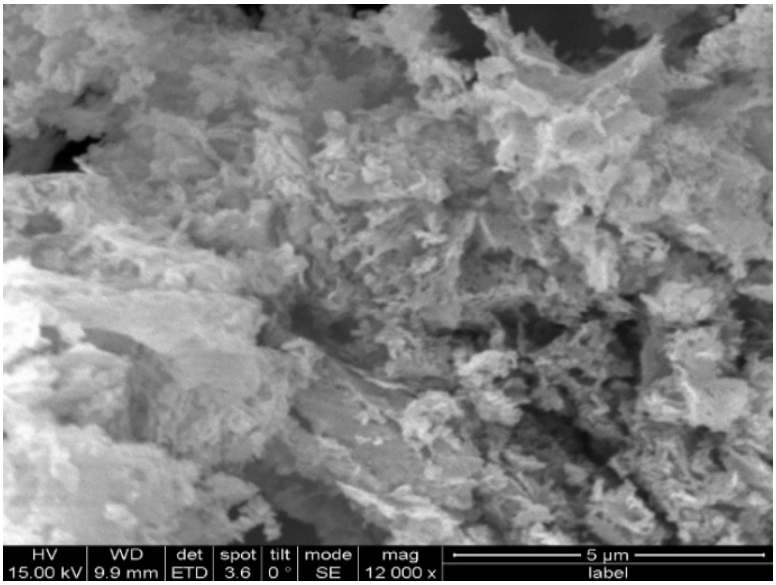

Figure 5. SEM micrograph of the nanopowder

3.4. *Band gap energy measurements*

Figure 6 shows the plot for determination of the band gap energy of the nanopowder. The value of E_g was found to be 2.22 eV which matched well with the one reported in the literature for α-Fe_2O_3 [54].

3.5. *Photocatalytic activity of the nanopowder*

The effect of dosage of the nanopowder on the rate of photocatalytic removal of AO 7 is depicted in Figure 7. The percentage dye removal increased with increase in the amount of the nanopowder. This is because an increase in the amount of the nanopowder resulted in an increase in the number of active sites available for adsorption of the dye molecules on its surface. In case of 10 and 20 ppm dye solutions, the optimum dosage was found to $1.2gL^{-1}$ whereas it was $1.4gL^{-1}$ for 40 and 60 ppm solutions. When the dosage of the nanopowder increased beyond the optimum value, the percentage dye removal was found to be negligible. This is due to the fact that higher concentration of the photocatalyst increased the scattering of the UV radiation. Additionally, it also decreased the penetration of the Uv radiation into the dye solution.

Figure 8 represents the effect of irradiation time on the rate of photocatalysis. The optimum irradiation time in case of 10 and 20 ppm dye solutions was found to be 45 minutes against the 50 minutes for 40 and 60 ppm dye solutions. The percentage dye removal was negligible beyond the irradiation time.

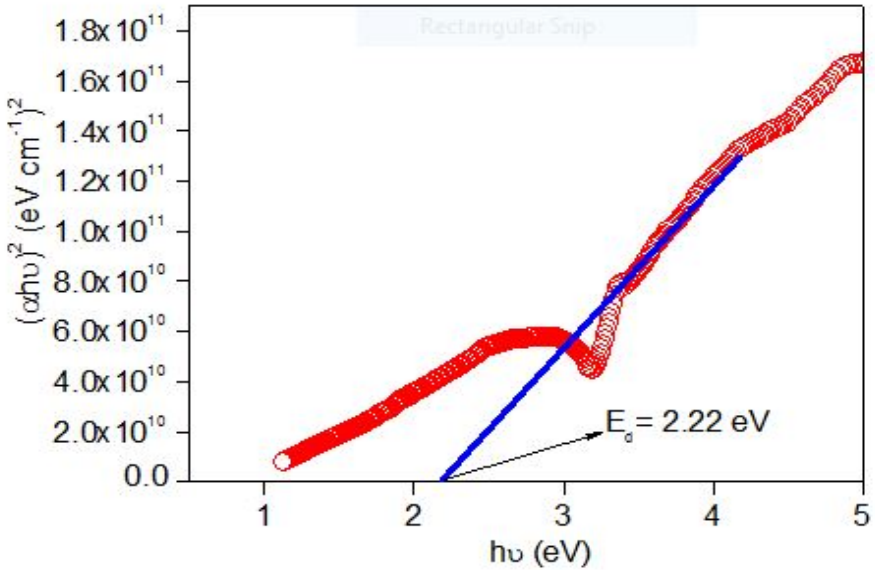

Figure 6. Band gap energy of the nanopowder.

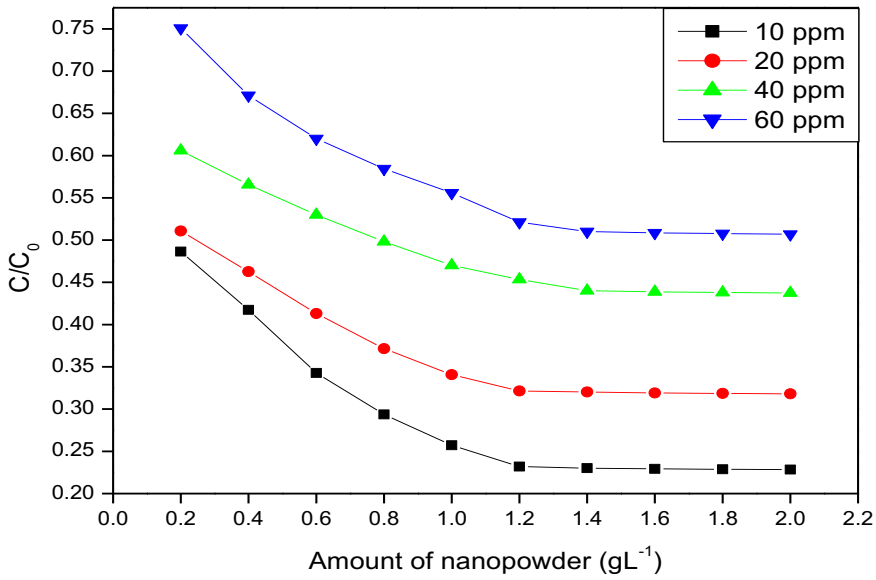

Figure 7. Effect of dosage of photocatalyst

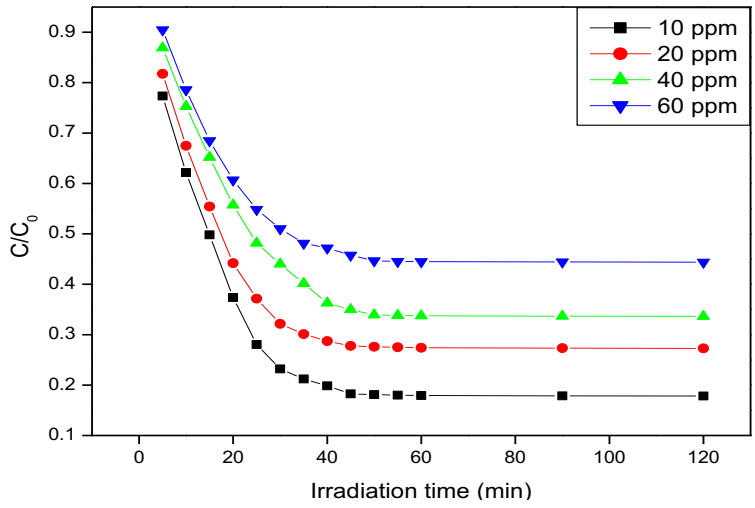

Figure 8. Effect of irradiation time

Conclusions

α-Fe_2O_3 nanopowder was successfully synthesized by solution combustion method and characterized by PXRD, FTIR, SEM, band-gap energy and BET surface area. The nanopowder acted as good photocatalyst for the removal of acid orange 7 dye from its aqueous solution. The rate of photocatalytic dye removal decreased with increase in initial concentration of the dye solution.

Acknowledgements - The authors gratefully acknowledge the support rendered by the TEQIP Laboratory of M.S. Ramaiah Institute of Technology, Bangaloreby providing the facilities to carry out the research work. MNZA is thankful to Dr. Sanaulla P.F, Head, Department of Chemistry, the Principal and Management of HKBK College of Engineering, Bangalore for encouragement and support. Thanks are due to Dr. Syed Abu Sayeed Mohammed, Head, Department of Civil Engineering, HKBK College of Engineering, Bangalore for giving useful suggestions and encouragement.

References

1. Ashly Leena Prasad, Thirumalisamy Santhi, *Sustain. Environ. Res.* 22 (2) (2012) 113.
2. Hazrat A., Muhammad S.K., *Environ. Sci. Technol.* 1 (3) (2008) 143.
3. AdmasuAdamu, Adsorptive Removal of Reactive Azo Dyes using IndustrialResidue, 2008, Ph.D. thesis.
4. Aksu, Z., *J. Process Biochem.*40 (2005) 997.
5. Robinson T., Chandran B., Nigam, P., *J. Env. Inter.*28 (2002) 29.
6. Inoue K., Yoshida M., Takahashi M., Fujimoto H., Ohnishi K., Nakashima K., Shibutani M., Hirise M., Nishikawa A., *Food Chem. Toxicol.* 47 (2009) 752.
7. Carlos A.M., Enric B., 2009. Decontamination of wastewaters containing synthetic organic dyes by electrochemical methods: A general review. App. Catal. B : Environ. 87 (3-4), 105-145.
8. Soni B.D., Ruparelia J.P, *J. Environ. Res. Dev.* 6 (4) (2012) 973.
9. Bayramoglu G., Arica, M.Y., *J. Hazard. Mater.*143 (2007) 137.
10. Iscen C.F., KiranI., IlhanS., *J. Hazard. Mater.*143 (2007) 335.
11. Parag A. Deshpande, Giridhar Madras, *Chemical Engineering Journal* 158 (2010) 571.
12. Ponnusamy Sivakumar, NachimuthuPalanisamy, *Advances in Applied ScienceResearch,* 1(1) (2010) 58.
13. Safavi A., SedaghatiF., Highly efficient degradation of azo dyes by carbon nanocrystals in the presence of hydrogen peroxide, Proceedings of the 4th International Conference on Nanostructures (ICNS4). Kish Island, I.R. Iran. March12-14, 2012.
14. Kayan B., Gözmen B., Demirel M., Gizir A.M., *J. Haz. Mater.* 177 (2010) 95.
15. Crini G., *J. Bioreso. Technol.*97 (2006) 1062.
16. Panizza M., Cerisola G., *Ind. Eng. Chem. Res.*47 (18) (2008)6816.
17. Hu Y.S., Kleiman-Shwarsctein A., Forman A.J., Hazen D., Park, J.N., McFarland, E.W., *Chem. Mater.* 20 (2008) 3805.
18. Cesar I., Kay A., Martinez J.A.G., Gratzel M., *J. Am. Chem. Soc.* 128 (2006) 4582.
19. Zhong D.K., Sun J.W., Inumaru H., Gamelin D.R., *J. Am. Chem. Soc.* 131 (2209) 6086.
20. Zhonghai Zhang, Mohammed FarukHossain, Takakazu Takahashi, *Applied Catalysis B: Environmental* 95 (2010) 423.
21. Lili Li, Ying Chu, Yang Liu, Lihong Dong, *J. Phys. Chem. C* 111 (2007) 2123.
22. Liu L., Kou H.Z., Mo W.L., Liu H.J., Wang, Y.Q., *J. Phys. Chem. B* 110 (2006) 15218.
23. Rajesh Kumar, Gautam, S., In-Chul Hwang, Jae Rhung Lee, Chae, K.H., Nagesh Thakur, *Mater. Lett.* 63 (2009) 1047.
24. Bell A.T., *Science* 299 (5613) (2003) 1688.
25. Huo L.H., Li W., Luc L., Cui H., Xi S.Q., Wang J., Zhao B., Shen Y.C., Lu Z.H., *Chem. Mater.*12 (2000) 790-794.
26. Wu C., Yin P., Zhu X., Ou Yang C., Xie Y., *J. Phys. Chem. B* 110 (2006) 17806.
27. Wen X. G., Wang S. H., Ding Y., Wang Z. L., Yang S., *J. Phy. Chem. B* 109 (1) (2005) 215.
28. Jia C.J., Sun L.D., Yan Z.G., You L.P., Luo F., Han X.D., Pang Y.C., Zhang Z., Yan C.H., *Angew. Chem. Int. Ed.* 44 (2005.) 4328.
29. Zhu L. P., Xiao H.M., Liu X.M., Fu S.Y., *J. Mater. Chem.* 16 (2006) 1794.
30. Zheng Y.H., Cheng Y., Wang Y.S., Bao F., Zhou L.H., Wei X.F., Zhang Y.Y., Zheng Q., *J. Phys. Chem. B* 110 (2006) 3093.
31. Tang B., Wang G., Zhuo L., Ge J., Cui, L., *J. Inorg. Chem.* 45 (2006) 5196.
32. Mao B., Kang Z., Wang E., Tian C., Zhang Z., Wang C., Song Y., Li M., *J. Solid State Chem.* 180 (2) (2007) 489.

33. Pu Z.F., Cao M.H., Yang J., Huang K.L., Hu C.W., *Nanotechnology*17 (2006) 779.
34. Khedr M.H., Abdel Halim K.S., Soliman N.K., *Materials Letters* 63 (2009) 598.
35. Cornell R.M., SchwertmannU., *The iron oxides* VCH, NewYork 1996.
36. Seip C.T., O'ConnorC.J., *Nanostruct. Mater.* 12 (1999) 183.
37. Zhang D.E., TongZ.W., LiS.Z., ZhangX.B., YingA.L., *Mater. Lett.* 62(24) (2008) 4053.
38. Jiang W.Q., YangH.C., YangS.Y., HorngH.E., HungJ.C., ChenY.C., HongC.Y., *J. Magn. Magn. Mater.* 283 (2004) 210.
39. Xu J., Yang H.B., Fu W.Y., Du K., Sui Y.M., Chen J.J., Zeng Y., Li M.H., Zou G.G., *J. Magn. Magn. Mater.* 309 (2) (2007) 307.
40. Wu M.Z., XingY., JiaY.S., NiuH.L., QiH.P., YeJ., ChenQ.W., *Chem. Phys.Lett.* 401 (2005) 374.
41. Mimani T., PatilK.C., *Mater. Phys. Mech.* 4 (2001) 134.
42. Aruna S. T., MukasyanA. S., *Current Opinion in Solid State and Materials Science*12 (2008) 44.
43. Patil K.C., HegdeM.S., TanuR., ArunaS.T., *Chemistry of nanocrystalline oxide materials: combustion synthesis, properties and applications,* World Scientific, Singapore, p 332, 2008.
44. Zulfiqar Ahmed M.N., Chandrasekhar K.B., Jahagirdar A.A., Nagabhushana H., Nagabhushana B.M., *Appl. Nanosci*. 5 (2015) 961.
45. MadhusudhanaN., KambalagereY., KittappaM.M., *Res. J. Chem. Sci.* 2 (2012) 72.
46. Tsunekawa S., FukudaT., KasuyaA., *J. Appl. Phys.* 87 (2000) 1318.
47. Gupta V.K., Mittal A., Gajbe V., Mittal J., *Industrial and Engineering Chemistry Research* 45 (4) (2006) 1446.
48. Joaquim Pedro Silva, Sonia Sousa, Jose Rodrigues, Helena Antunes, John J. Porter, Isolina Goncalves, Suzana Ferreira-Dias, *Separation and Purification Technology* 40 (3) (2004) 309.
49. Lei Zhang, Zhengjun Cheng, Xiao Guo, Xiaohui Jiang, Rong Liu, *Journal of Molecular Liquids* 197 (2014) 353.
50. Loghman Karimi, Salar Zohoori, Mohammad Esmail Yazdanshenas, *Journal of Saudi Chemical Society* 18 (2014) 581.
51. Hua J., Gengsheng J., *Mater. Lett.* 63 (2009) 2725.
52. Jahagirdar A.A., Dhananjaya N., Monika D.L., Kesavulau C.R., Nagabhushana H., Sharma S.C., Nagabhushana B.M., Shivakumara C., Rao J.L., Chakradhar R.P.S., *Spectrochimica Acta Part A: Molecular and Biomolecular Spectroscopy* 104(2013) 512.
53. Bourdjiba O., Bekkouche F., Hassaine A., Djenidi R., *Eur. J. Sci. Res.* 26 (2009) 80.
54. Kroell M., Pridoehl M., Zimmermann G., Pop L., Obendach S., Hartwig A., *J. Magnetism and Magnetic Materials* 289 (2005) 21.

(2018) ; http://www.jmaterenvironsci.com